

Electron correlation and the self-interaction error of density functional theory

VICTOR POLO, ELFI KRAKA and DIETER CREMER*

Department of Theoretical Chemistry, Göteborg University, Reutersgatan 2,
S-41320 Göteborg, Sweden

(Received 12 July 2001; accepted 8 November 2001)

The self-interaction error (SIE) of commonly used DFT functionals has been systematically investigated by comparing the electron density distribution $\rho(\mathbf{r})$ generated by self-interaction corrected DFT (SIC-DFT) with a series of reference densities obtained by DFT or wavefunction theory (WFT) methods that cover typical electron correlation effects. Although the SIE of GGA functionals is considerably smaller than that of LDA functionals, it has significant consequences for the coverage of electron correlation effects at the DFT level of theory. The exchange SIE mimics long range (non-dynamic) pair correlation effects, and is responsible for the fact that the electron density of DFT exchange-only calculations resembles often that of MP4, MP2 or even CCSD(T) calculations. Changes in the electron density caused by SIC-DFT exchange are comparable with those that are associated with HF exchange. Correlation functionals contract the density towards the bond and the valence region, thus taking negative charge out of the van der Waals region where these effects are exaggerated by the influence of the SIE of the correlation functional. Hence, SIC-DFT leads in total to a relatively strong redistribution of negative charge from van der Waals, non-bonding, and valence regions of heavy atoms to the bond regions. These changes, although much stronger, resemble those obtained when comparing the densities of hybrid functionals such as B3LYP with the corresponding GGA functional BLYP. Hence, the balanced mixing of local and non-local exchange and correlation effects as it is achieved by hybrid functionals mimics SIC-DFT and can be considered as an economic way to include some SIC into standard DFT. However, the investigation shows also that the SIC-DFT description of molecules is unreliable because the standard functionals used were optimized for DFT including the SIE.

1. Introduction

In the last decade, density functional theory [1–3] has become one of the most used correlation corrected quantum chemical methods [4]. Clearly, this is a result of its wide applicability and reliability [4], reflected in the fact that it meets the performance of second-order Møller–Plesset (MP2) perturbation theory [5, 6], fourth-order MP (MP4) [6] or even coupled cluster methods such as CCSD(T) [7–10]. However, while wavefunction theory (WFT) methods systematically introduce correlation effects in a stepwise manner, DFT covers dynamic electron correlation in an unspecified way, which makes it difficult to predict the outcome of a DFT calculation unless DFT results for a closely related reference system are known.

In recent work, Cremer and coworkers [11] investigated electron correlation effects covered by DFT by comparing its electron density distribution $\rho(\mathbf{r})$ with that of a WFT method, which covers well defined electron correlation effects. Such a comparison is best done

with the help of the difference electron density distribution $\Delta\rho(\mathbf{r}) = \rho(\text{DFT}) - \rho(\text{WFT})$ [12, 13]. In this way a global impression of electron correlation effects is obtained that is more informative than analysing single values of selected molecular properties such as energy, geometry, etc. Cremer and coworkers [11] showed that dynamic electron correlation effects reminiscent of pair and three-electron correlation effects introduced by MP2 and MP4 in WFT are largely mimicked by the DFT exchange (X) functionals. If one uses GGA (generalized gradient approximation) exchange functionals, the best agreement between exchange only and WFT calculations will be found at MP4 while MP2 and CCSD(T) show also large similarities with exchange only results [11]. Correlation (C) functionals introduce corrections in the electron density distribution that are typical of the coupling between diagonal (2-, 3-, etc.) electron correlation effects included in higher order MP_n and CC methods [14–19], i.e. DFT correlation functionals contain by their construction correlation effects not (or only partially) covered by low order MP_n methods [11].

* Author for correspondence. e-mail: cremer@theoc.gu.se

Since electron correlation is differently defined at the DFT and WFT levels of theory [1–3, 11], it is not necessarily contradictory that dynamic correlation effects introduced by low order MP n methods seem to be already covered by X-DFT functionals. However, considering the construction of the exchange functionals there is no obvious reason why they should cover, e.g. typical pair electron correlation effects. Therefore, we shall investigate in this work the self-interaction of the electrons as one of the possible effects influencing the performance of exchange but also correlation functionals. In this way, we seek a deeper understanding of how electron correlation is covered by standard DFT methods.

In WFT methods, the form of the many-particle Hamiltonian guarantees that an electron interacts with other electrons but does not interact with itself. Actually, the self-interaction term included by the Coulomb potential is exactly cancelled out by a similar term in the exchange potential. Because exchange is treated by commonly used exchange functionals only in an approximate way, Coulomb self-interaction and exchange self-interaction of an electron no longer cancel at the DFT level and lead to a self-interaction error (SIE) [3, 20–26]. The reason for the existence of an exchange self-interaction error (X-SIE) is obvious, but there is also a correlation self-interaction error (C-SIE) which results from the fact that most (but not all) correlation functionals predict for a single electron a negative correlation energy. The SIE has been investigated since the early days of DFT [27], and methods have been suggested to cure DFT from an XC-SIE [21–27]. In this work, a self-consistent field formulation [24] of the self-interaction correction (SIC) given by Perdew and Zunger [21, 22] is used to investigate the effects of the SIE of common XC functionals on the electron density distribution. In this connection, we shall discuss the following questions. (1) How does the SIE influence the performance of commonly used exchange functionals? Is it possible that the SIE simulates specific correlation effects covered by correlation corrected WFT methods? (2) How does the C-SIE affect the electron density distribution and how is this reflected in the performance of standard correlation functionals? (3) Does SIC-DFT cover more (or fewer) Coulomb correlation effects than standard DFT and, if so, does this lead to an improvement (deterioration) in the performance of commonly used exchange–correlation functionals? (4) How can the SIE be related to well known features of the exchange–correlation hole? (5) In view of the relatively high cost of SIC-DFT are there other less expensive ways of correcting DFT for SIEs?

To answer these questions, this work is structured in the following way. First, we shall review the theory of

SIC-DFT and describe the computational details of the calculations carried out in this work. In §3 we establish and classify correlation effects with the help of MP and CC theory. In §4 the X-SIEs and C-SIEs of commonly used exchange–correlation functionals will be analysed using appropriate WFT references, and DFT hybrid functionals will be analysed in §5.

2. Computational methods

In standard Kohn–Sham (KS) DFT [1–3] the electronic energy of the ground state of an atom or molecule,

$$E[\rho] = E_T[\rho] + E_V[\rho] + E_J[\rho] + E_X[\rho] + E_C[\rho], \quad (1)$$

is given as a functional of the electron density distribution

$$\rho(\mathbf{r}) = \sum_{\sigma} \rho_{\sigma}(\mathbf{r}) = \sum_{\sigma} \sum_{i=1}^{N_{\sigma}} \rho_{i\sigma}(\mathbf{r}) = \sum_{\sigma} \sum_{i=1}^{N_{\sigma}} |\varphi_{i\sigma}(\mathbf{r})|^2, \quad (2)$$

where σ denotes α (up) or β (down) spin, N_{σ} the number of α or β electrons and by this the number of occupied α or β KS spin orbitals φ_i . In equation (1), $E_T[\rho]$, $E_V[\rho]$, $E_J[\rho]$, $E_X[\rho]$, and $E_C[\rho]$ have the usual meaning of the kinetic energy of non-interacting electrons:

$$E_T[\rho] = \sum_{\sigma=\alpha,\beta} \sum_{i=1}^{N_{\sigma}} \langle \varphi_{i\sigma} | -\frac{1}{2} \nabla^2 | \varphi_{i\sigma} \rangle, \quad (3)$$

the electron–nuclear attraction energy described by the external potential $v(\mathbf{r})$,

$$E_V[\rho] = \int d\mathbf{r} \rho(\mathbf{r}) v(\mathbf{r}), \quad (4)$$

the Coulomb interaction energy,

$$E_J = -\frac{1}{2} \int d\mathbf{r} d\mathbf{r}' \frac{\rho(\mathbf{r})\rho(\mathbf{r}')}{|\mathbf{r} - \mathbf{r}'|}, \quad (5)$$

the exchange energy $E_X[\rho_{\alpha}, \rho_{\beta}]$, and the correlation energy $E_C[\rho_{\alpha}, \rho_{\beta}]$, respectively.

Both exchange and correlation functionals of any SIC-DFT [21–23] must fulfil equations (6)–(9), which describe their values in the limit of a one-electron density $\rho_{\sigma}(\mathbf{r})$ where σ may be α , $\int \rho_{\alpha}(\mathbf{r}) d\mathbf{r} = 1$, and $\rho_{\beta}(\mathbf{r}) = 0$.

$$E_J[\rho] + E_X[\rho_{\sigma}, 0] = 0, \quad (6)$$

$$E_C[\rho_{\sigma}, 0] = 0, \quad (7)$$

$$v_J([\rho]; \mathbf{r}) + v_X^c([\rho_{\sigma}, 0]; \mathbf{r}) = \text{const}, \quad (8)$$

$$v_C^c([\rho_{\sigma}, 0]; \mathbf{r}) = 0. \quad (9)$$

Equation (6) expresses that a single electron does not interact with itself, i.e. the self-repulsion energy of the

electron contained in $E_J[\rho]$ is cancelled by the self-exchange energy covered by the exchange functional. Equation (7) clarifies that a single electron does not possess any correlation energy (*self-correlation*) and equations (8) and (9) make sure that the single electron moves under the influence of the external potential $v(\mathbf{r})$ rather than the Coulomb potential v_J , the exchange potential v_X or the correlation potential v_C . An approximate exchange–correlation functional may violate all or some of the equations (6)–(9) and, therefore, has to be corrected.

The SIC-DFT method proposed by Perdew and Zunger [21] for LDA (local density approximation) functionals, but also used for GGA functionals [22] remedies the SIE orbital by orbital.

$$\begin{aligned} E_X^{\text{correct}} &= E_X^{\text{approx}}[\rho_\alpha, \rho_\beta] \sum_{\sigma=\alpha,\beta} \sum_i^{N_\sigma} (E_J[\rho_{i\sigma}] + E_X^{\text{approx}}[\rho_{i\sigma}, 0]) \\ &= E_X^{\text{approx}}[\rho_\alpha, \rho_\beta] - E_X^{\text{SIC}}, \end{aligned} \quad (10)$$

$$\begin{aligned} E_C^{\text{correct}} &= E_C^{\text{approx}}[\rho_\alpha, \rho_\beta] - \sum_{\sigma=\alpha,\beta} \sum_i^{N_\sigma} E_C^{\text{approx}}[\rho_{i\sigma}, 0] \\ &= E_C^{\text{approx}}[\rho_\alpha, \rho_\beta] - E_C^{\text{SIC}}. \end{aligned} \quad (11)$$

Hence, the electronic energy of SIC-DFT is given by equation (12).

$$\begin{aligned} E^{\text{SIC-DFT}}[\rho] &= E_T[\rho] + E_V[\rho] + E_J[\rho] + E_X[\rho] - E_X^{\text{SIC}}[\rho] \\ &\quad + E_C[\rho] - E_C^{\text{SIC}}[\rho] \end{aligned} \quad (12)$$

The energy of equation (12) must be made stationary with regard to a mixing of occupied with occupied and occupied with virtual orbitals, which is accomplished by solving the KS equations extended by the Perdew–Zunger SIC-XC functional [24]. The theory and implementation of a self-consistent SIC-DFT (SCF-SIC-DFT) method are described elsewhere [28]. SCF-SIC-DFT was used in this work to determine the electron density distribution of a series of molecules to analyse the SIE of standard exchange–correlation functionals.

Due to the mixing of occupied orbitals in the SCF-SIC-DFT procedure, the energy is no longer invariant with regard to orbital rotations among occupied orbitals. Previous work [29] demonstrated that localized orbitals minimize the SIC-DFT energy by maximizing the cancellation between Coulomb, exchange, and correlation self-interactions. This, however, leads to the problem that SCF-SIC-DFT densities and normal DFT densities are no longer directly comparable. In the SCF-SIC-DFT density, multiple bonds will be represented as bent bonds rather than σ – π bonds. We solved this problem by suppressing a mixing of σ and π orbitals in the SCF-SIC procedure. This was achieved by

excluding π orbitals from the localization procedure when generating difference density diagrams. This has a significant effect on the energy as is reflected in the calculated SCF-SIC-BLYP/cc-pVTZ energies obtained for ethene: $-78.514\,26\,E_h$ (full localization); $-78.503\,79\,E_h$ (π orbitals excluded from the localization). Although the partial localization procedure leads to errors in SCF-SIC-BLYP energies and other properties, it produces meaningful difference densities because the major part (78%) of the SIE ($-0.047\,02\,E_h$) is covered by this approach (see discussion of electron interaction energies in §3).

A series of small molecules representing typical bonding situations ($\text{H}-\text{H}$, $\text{H}_3\text{C}-\text{CH}_3$, $\text{H}_2\text{C}=\text{CH}_2$, $\text{HC}\equiv\text{CH}$, $\text{H}_2\text{N}-\text{NH}_2$, $\text{HN}=\text{NH}$, $\text{N}\equiv\text{N}$, $\text{O}=\text{O}$, $\text{HO}-\text{OH}$, $\text{F}-\text{F}$, CH_3-OH , $\text{H}_2\text{C}=\text{O}$, $\text{C}\equiv\text{O}$) were calculated at various DFT and SCF-SIC-DFT levels of theory where experimental geometries were employed throughout [30]. Reference densities were calculated using standard HF, MP [5, 6] and CC theories [7–10] with unfrozen core and analytical energy gradients [13]. The MP and CC response density distributions were calculated with procedures described elsewhere [12, 13]. All calculations were carried out with Dunning's cc-pVTZ basis set, which corresponds to a (10s5p2d1f/5s2p1d) [4s3p2d1f/3s2p1d] contraction [31].

A series of electron correlation effects was established in the following way (compare with table 1). DFT without any XC functional (DFT0), SIC-DFT0 = Hartree, and HF theory were used to demonstrate via the difference density $\Delta\rho(J_{\text{SI}}) = \rho(\text{DFT0}) - \rho(\text{Hartree})$ the impact of electron self-repulsion $J_{\text{SI}} = \sum J_{ii}$ and via $\Delta\rho(\text{exchange}) = \rho(\text{HF}) - \rho(\text{Hartree})$ the influence of exact exchange interactions $\sum K_{ij}$ (table 1, entries 1 and 2). Of course, the difference densities are determined by using different orbitals in the first method and the second method, so that other effects are also covered by the difference densities. However, the major influence should be that of electron self-repulsion and exchange interactions, which justify the use of short notations such as exchange density distribution for the difference density given by entry 2 in table 1, although the exact exchange energy density distribution would have to be defined in a different way [32].

The difference between MP2 and HF densities illustrates the effects of electron pair correlation as covered by the D excitations. Since the latter are not coupled, pair correlation effects are largely exaggerated at the MP2 level of theory, which is partially corrected at MP3 by a coupling between D excitations (table 1). MP4 introduces orbital relaxation effects (via the S excitations), three-electron correlation effects (via T excitations), and disconnected four-electron correlation effects via Q excitations. Higher order correlation

Table 1. Electron interaction effects studied at various levels of theory.^a

	Difference density $\Delta\rho(\mathbf{r}) = \rho(\text{method I}) - \rho(\text{method II})$	Electron interaction effects studied	Theoretical Terms Covered
1	DFT0-Hartree	Coulomb self-interaction	$(\sum J_{ij} + \sum J_{ii}) - (\sum J_{ij})$
2	HF-Hartree	HF (correct) exchange	$\sum (J_{ij} - K_{ij}) - (\sum J_{ij})$
3	MP2-HF	pair correlation effects	D excitations
4	MP3-MP2	coupling between pair correlation effects	DD' excitations
5	MP4(SDQ)-MP3	orbital relaxation, disconnected 4-electron correlation effects	S and Q excitations
6	MP4-MP4(SDQ)	three-electron correlation	T excitations
7	CCSD-MP4(SDQ)	infinite order correlation effects in the SD space	T excitations
8	CCSD(T)-CCSD	77% of the infinite order three-electron correlation effects	TT, TD, etc.
9	[CCSD(T)-CCSD]-[MP4-MP4(SDQ)]	coupling of T effects and infinite order T effects space	X-SIE
10	X-(SIC-X)	exchange self-interaction error	$(\sum (J_{ij} - X_{ij}) - \sum J_{ij})$
11	(SIC-X)-Hartree	correct DFT exchange	$\sum (J_{ij} - X_{ij}) - \sum (J_{ij} - K_{ij})$
12	(SIC-X)-HF	difference in exchange interactions	C functional
13	XC-X	dynamic correlation effects	C-SIE
14	(HF+O)-(HF+SIC-C)	correlation self-interaction error	SIC-C
15a	(SIC-XC)-(SIC-X)	correct correlation effects without C-SIE	SIC-C
15b	(HF+SIC-C)-HF	correct correlation effects without C-SIE	SIC-C
15c	[XC-X]-[(HF+O)-(HF+SIC-C)]	correct correlation effects without C-SIE	SIC-C

^a Additional combinations were studied to determine the position of a particular method in figure 2. The following abbreviations are used:

Term	Explanation	Term	Explanation
X	DFT exchange (X: S, B, PW91, etc.)	C-SIE	self-interaction error of the correlation functional
C	DFT correlation (C: VWN, VWN5, LYP, PW91, etc.)	SIC	self-interaction corrected
XC	exchange-correlation (SVWN, BLYP, PW91/PW91, etc.)	SIC-X	self-interaction corrected exchange functional
SIE	self-interaction error	SIC-C	self-interaction corrected correlation functional
X-SIE	self-interaction error of the exchange functional	DFT0	DFT without XC functional

effects as they are introduced at fifth-order (MP5) and sixth-order MP theory (MP6) [14–16] cannot be described because analytical gradients for calculating response densities are not available. Although MP theory is problematic in its application because of frequent initial oscillations in the MP n series [17], it provides a platform for analysing electron correlation effects [18, 19] covered by more advanced methods such as CCSD [9] or CCSD(T) [10]. CCSD contains infinite-order orbital relaxation and pair correlation effects in the SD space, which become obvious when comparing CCSD and MP4(SDQ) densities (table 1). CCSD(T) covers (up to MP8) 77% of the terms of the SDT space of the more complete CCSDT method [19]. Important TT coupling effects can be studied when comparing three-electron correlation effects at MP4 and CCSD(T) with the help of the difference density electron density distribution $[\rho(\text{CCSD(T)}) - \rho(\text{CCSD})] - [\rho(\text{MP4}) - \rho(\text{MP4(SDQ)})]$ (table 1).

The DFT functionals employed reach from LDA to GGA and hybrid functionals (for details, see [11]). Because of space limitations we give for each class of functionals just one or two representatives, namely the SVWN5 functional [33, 34] as a typical LDA functional, the BLYP [35, 36] and PW91P91 functionals [37] as typical GGA functionals and the B3LYP functional [38] as the typical and most often used hybrid functional. The electron interaction effects caused by X-SIE were obtained by comparing SIC-X calculations with exchange only calculations. The SIC-C was investigated in different ways, viz. (a) by comparing SIC-XC with SIC-X densities, (b) with the help of the difference density generated from HF+SIC-C and HF calculations, and (c) from the difference density distribution defined by $[\rho(\text{XC}) - \rho(\text{X})] - [\rho(\text{HF} + \text{C}) - \rho(\text{HF} + \text{SIC} - \text{C})]$. Procedures (a), (b), and (c) use different orbitals and thus they should lead to differing SIC-C densities. However, the difference density plots obtained by the three approaches agree qualitatively, so that in the following discussion there is no need to distinguish between SIC-C density distributions obtained in different ways.

Calculations were performed with the quantum chemical program packages Cologne2000 [39], Gaussian98 [40], and Aces II [41].

3. Analysis of the electron density distributions calculated with SCF-SIC-DFT

In this work, only a limited number of the difference density plots calculated can be represented and discussed. We select ethene as a representative example that shows effects typical of single and multiple bonded systems. In the following, we simplify the discussion by using the term SIC-DFT rather than SCF-

SIC-DFT. Also, we distinguish between a method such as SIC-DFT, SIC-XC, SIC-X based on an SIC-XC, etc., functional and the errors X-SIE, C-SIE or XC-SIE, which are related to the corrections X-SIC = $-(\text{X-SIE})$, etc. First, we clarify the magnitude of calculated SIEs for some typical examples using the electron interaction energies summarized in table 2.

3.1. Electron interaction energies

Since intraorbital electron interactions generally are larger than interorbital interactions, self-Coulomb and self-exchange interactions represent a large fraction of the total Coulomb (HF, 16%) and exchange interaction energy (HF, more than 90%, table 2). For the LDA functional SVWN5, the S-SIE = $\sum(J_{ii} - X_{ii})$ is relatively large and always positive because of the underestimation of exchange interactions by the S functional. In the case of H₂, the S-SIE corresponds to more than twice the correlation energy ($0.041 E_h$).

For H₂, C-SIE is of opposite sign, thus exaggerating its correlation energy by almost a factor of 2. Although the X-SIE and C-SIE cancel each other partially, the total SIE is almost as large as the correct SVWN5 correlation energy of H₂ ($0.04932 E_h$, table 2). In this way the SIE has the same impact on the total energy as the correlation error has in WFT theory.

GGA functionals improve the situation in so far as the X-SIE is strongly reduced (PW91-exchange, $0.01009 E_h$ for H₂, table 2), resulting from the fact that exchange interactions are increased by a GGA X-functional such as PW91. The correlation part is also improved and the C-SIE reduces to $-0.01472 E_h$ for H₂; hence the total SIE becomes negative ($-0.00463 E_h$) its value being just 15% of the correct PW91 correlation energy of H₂ ($-0.03133 E_h$, table 2).

In the case of the BLYP functional, the XC-SIE for H₂ is even smaller because the LYP functional by construction does not suffer from a C-SIE. However, in general the total SIE values resulting from the PW91PW91 GGA functional are at least a factor of 2 smaller in magnitude than those obtained with the BLYP functional, which clearly is a result of the different signs of the X-SIE (> 0) and the C-SIE (by definition < 0) in the case of PW91. However, the negative XC-SIE obtained with BLYP is still a small fraction of the relatively large positive XC-SIE of LDA functionals. Hence, one could draw the conclusion that the SIE is a problem of only LDA rather than GGA functionals. Closer inspection, however, reveals that even for the PW91PW91 functional the C-SIE is about $9 mE_h$ per electron pair, which still leads to substantial errors in the molecular energy. This is confirmed when analysing the influence of XC-SIEs on the electronic structure of a molecule such as ethene.

Table 2. Electron interaction energies for four molecules calculated at various levels of theory.^a

Molecule	XC functional	J	$\sum J_{ii}$	X	$\sum X_{ii}$	X-SIE	X_{correct}	C	C-SIE	C_{correct}	XC	Total SIE	XC_{correct}	E_{ee}
H ₂	HF	1.31634	0.65817	-0.65817	-0.65817	0	-0.65817	0	0	0	-0.65817	0	-0.65817	0.65817
	SVWN5	1.32532	0.66266	-0.57046	-0.57046	0.09220	-0.66266	-0.09508	-0.04575	-0.04932	-0.66554	0.04645	-0.71198	0.65978
	BLYP	1.32033	0.66017	-0.65706	-0.65706	0.00311	-0.66017	-0.03835	0	-0.03835	-0.69541	0.00311	-0.69852	0.62493
	PW91PW91	1.32197	0.66099	-0.65089	-0.65089	0.01009	-0.66099	-0.04605	-0.01472	-0.03133	-0.69694	-0.00463	-0.69231	0.62503
H ₂ C = CH ₂	HF	70.30410	11.16617	-11.74227	-11.16617	0	-11.74227	0	0	0	-11.74227	0	-11.74227	58.56183
	SVWN5	70.86286	11.19593	-10.57128	-9.67787	1.51806	-12.08934	-0.98908	-0.44839	-0.54069	-11.56036	1.06967	-12.63003	59.30249
	BLYP	70.46832	11.20597	-11.75897	-11.25300	-0.04702	-11.71195	-0.49770	0	-0.49770	-12.25667	-0.04702	-12.20965	58.21165
	PW91PW91	70.57834	11.19436	-11.73433	-11.06825	0.12611	-11.86044	-0.53037	-0.13366	-0.39671	-12.26470	-0.00755	-12.25715	58.31364
CO	HF	76.26343	12.34137	-13.33118	-12.34137	0	-13.33118	0	0	0	-13.33118	0	-13.33118	62.93226
	SVWN5	76.69274	12.38762	-12.08354	-10.76259	1.62503	-13.70856	-0.95190	-0.42614	-0.52576	-13.03544	1.19889	-14.23433	63.65730
	BLYP	76.22785	12.37729	-13.38372	-12.54786	-0.17058	-13.21315	-0.48446	0	-0.48446	-13.86818	-0.17058	-13.69761	62.35967
	PW91PW91	76.35125	12.37537	-13.36922	-12.33826	0.03712	-13.40634	-0.48811	-0.11169	-0.37643	-13.85734	-0.07457	-13.78277	62.49391
N ₂	HF	74.76418	12.17590	-13.10458	-12.17590	0	-13.10458	0	0	0	-13.10458	0	-13.10458	61.65960
	SVWN5	75.30582	12.22671	-11.89658	-10.61930	1.60741	-13.50399	-0.94754	-0.42363	-0.52392	-12.84413	1.18378	-14.02790	62.46170
	BLYP	74.85907	12.21923	-13.18578	-12.37949	-0.16025	-13.02553	-0.48313	0	-0.48313	-13.66891	-0.16025	-13.50865	61.19016
	PW91PW91	74.99327	12.21842	-13.17270	-12.17312	0.04530	-13.21800	-0.49065	-0.11411	-0.37654	-13.66335	-0.06882	-13.59453	61.32992

^a All energies are given in hartree. All calculations with the cc-pVTZ basis set at experimental geometries. J denotes the Coulomb interaction energy, $\sum J_{ii}$ the self-interaction energy, X the exchange energy, $\sum X_{ii}$ the self-exchange energy, $X - SIE$ the exchange self-interaction error, X_{correct} the correct DFT exchange energy obtained after correcting for the X-SIE, C the correlation energy, $C - SIE$ the correlation self-interaction error, C_{correct} the correct DFT correlation energy obtained after correcting for the C-SIE, XC the exchange-correlation energy, Total SIE the total self-interaction energy, XC_{correct} the correct exchange-correlation energy obtained after correcting for X-SIE and C-SIE, and E_{ee} the total electron interaction energy.

3.2. Dynamic correlation effects covered by WFT methods

The electron density distribution $\rho(\mathbf{r})$ of ethene obtained at the HF level of theory is characterized by an accumulation of negative charge in the bond region (both σ and π parts) and in the inner parts of the valence regions of the C atoms. This leads to shielding of the nuclear charges, a reduction in nuclear–nuclear repulsion, and a relatively short CC bond length, which will decrease further if larger basis sets are used in the HF calculation. Dynamic electron correlation changes the HF electron density distribution of ethene substantially, as is shown by the difference density plots of figure 1.

MP2 introduces left–right, angular, and in–out pair correlation effects via D excitations, which lead to typical changes in the electron density distribution of ethene (figure 1(a)): density is moved out of the CC and CH bond regions closer to the C atoms as a result of strong left–right correlation, which decreases the bond density. At the same time, density is transferred into the non-bonded regions beyond and between the H atoms. The density in the van der Waals region increases, where this is clearly a result of in–out correlation. Left–right correlation is also strong in the π space ($\pi \rightarrow \pi^*$ excitations) and, as a consequence, the van der Waals region above the π bond is depleted in density (figure 1(b)). The results of angular correlation, which should transfer negative charge from σ to π orbitals and vice versa, are more difficult to assess because they are superimposed by left–right and in–out correlation effects.

In passing we note that terms such as dynamic, non-dynamic, near-degeneracy, left–right, in–out, angular, etc., correlation are used by different authors in different ways. For example, Handy and Cohen [42] suggested in a recent paper that one should distinguish between left–right (long range) and dynamic (short range) correlation effects where the first term replaces terms such as non-dynamic, static or near-degeneracy correlation. Although the authors give arguments for their choice [42], we prefer to stay within the usual terminology, namely to consider short range correlation as dynamic and long range correlation as non-dynamic (static or near-degeneracy). This implies that pair correlation effects (left–right correlation: admixture of excited configurations having antibonding instead of bonding orbitals occupied; angular correlation; admixture of excited configurations having π instead of σ orbitals occupied; in–out correlation: admixture of excited configurations having virtual orbitals with additional nodal spheres at the atoms occupied; see also [6]) can be both dynamic (many excited configurations involving strongly oscillating orbitals are included in the wavefunction, each with small weight) or non-dynamic (a limited number

of excited configurations involving weakly oscillating orbitals are included in the molecular wavefunction, each with a relatively large weight). Hence left–right correlation is covered by both (single-determinant) MP methods (preferentially as short range) and MCSCF methods (preferentially as long range). It is also noteworthy in this connection that (a) use of the terms dynamic, non-dynamic, etc., correlation serves a qualitative description of correlation effects and faces problems as soon as one wants to distinguish between these terms in a quantitative way [43], and (b) that methods generally considered to cover dynamic electron correlation effects (CI, MP, CC, etc.) also cover some non-dynamic correlation effects because methods considered to cover predominantly non-dynamic correlation effects (MCSCF, CASSCF, etc.) cover also some dynamic correlation effects (see, e.g. [43]).

It is well known that MP2 exaggerates pair correlation effects, thus overcorrecting the HF values of the molecular properties and leading to opposite extremes relative from HF results [6]. This is schematically indicated in figure 2, where the degree of left–right and in–out correlation is given for commonly used WFT and DFT methods. MP3 introduces a coupling between D excitations (table 1) and, accordingly, reduces the degree of pair correlation considerably (figure 1(c,d)). In this way, changes in the electron density distribution as well as in the molecular properties are corrected back into the direction of the corresponding HF values (figure 2).

In passing we note that changes in the π space (figure 1(b,d)) are parallel to those in the σ space of ethene. To simplify the discussion, we shall concentrate on the σ space in the following and discuss features of the π density only if they differ from those of the σ density.

The inclusion of S, D, and Q excitations at the MP4(SDQ) level of theory corrects $\rho(\mathbf{r})$ further back to the HF density (ethene, figure 1(e)) or, alternatively, introduces some more left–right and in–out correlation (e.g. in the case of CO or N₂). In any case the MP4(SDQ) density distribution is close to that of the MP3 density. This holds also for the CCSD density which, in contrast to MP4(SDQ), covers infinite-order orbital relaxation and pair correlation effects in the SD space and, therefore, should give a reliable account of pair correlation effects (figure 1(f)). In the case of ethene, CCSD indicates that there is actually less left–right correlation than predicted at either the MP4(SDQ) or the MP3 level of theory. For molecules with triple bonds, CCSD adds left–right correlation to that already covered by MP3, but the level stays below the degree of left–right correlation predicted by MP4(SDQ) (figure 2).

The inclusion of three-electron correlation effects via T excitations at the MP4 level increases the left–right and

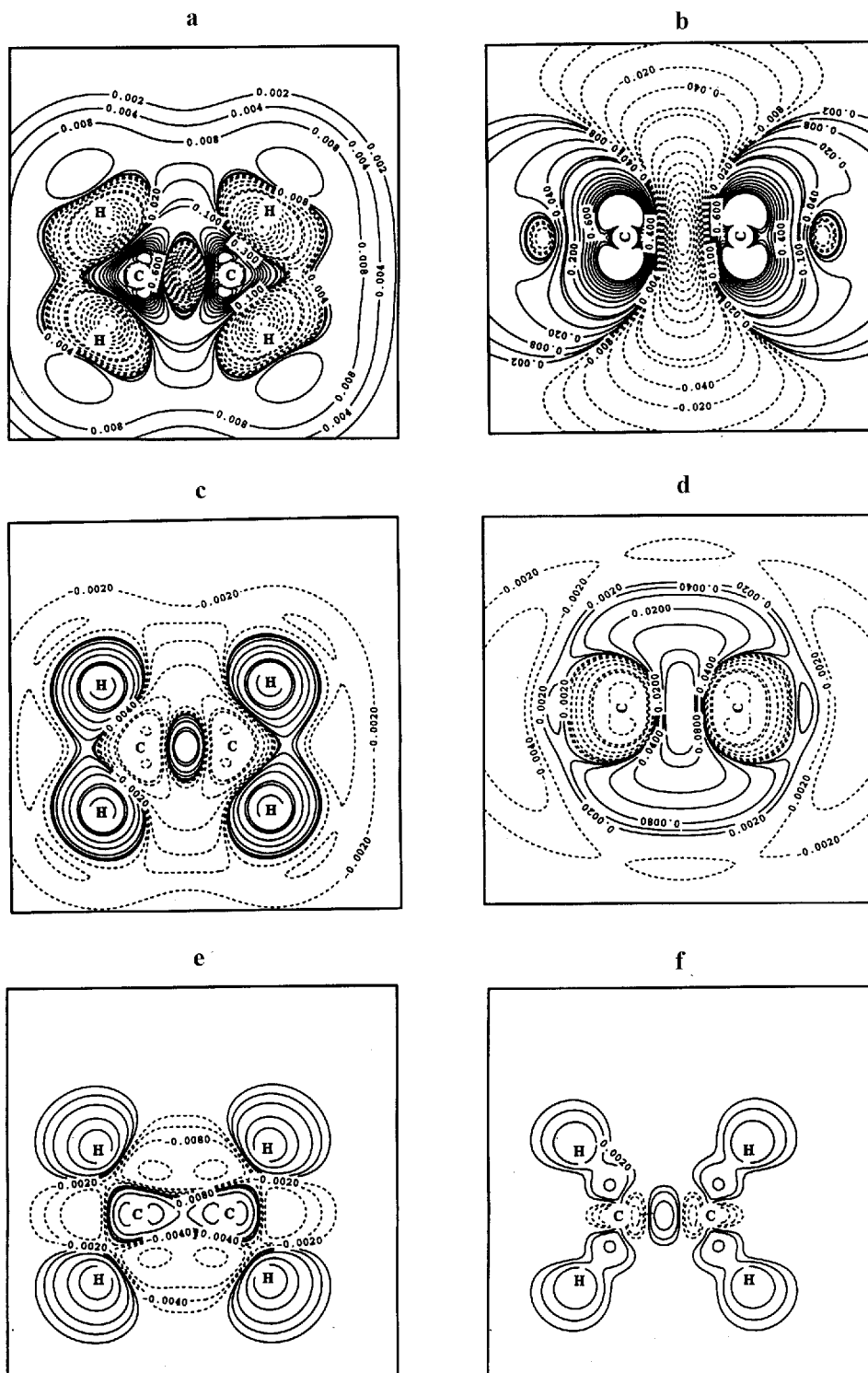


Figure 1. Contour line diagram of the difference electron density distribution $\Delta\rho(\mathbf{r}) = \rho(\text{methodI}) - \rho(\text{methodII})$ of ethene calculated with the cc-pVTZ basis in the experimental geometry. Solid (dashed) contour lines are in regions of positive (negative) difference densities. Reference plane, if not otherwise indicated, is the plane containing the atoms. The positions of the atoms are indicated. The contour line levels have to be multiplied by the scaling factor 0.01 and are given in $e a_0^{-3}$. (a) MP2-HF; (b) MP2-HF (plane perpendicular to the molecular plane and containing the C atoms); (c) MP3-MP2; (d) MP3-MP2 (plane perpendicular to the molecular plane and containing the C atoms); (e) MP4(SDQ)-MP3; (f) CCSD-MP4(SDQ); (g) MP4-MP4(SDQ); and (h) [CCSD(T)-CCSD]-[MP4-MP4(SDQ)].

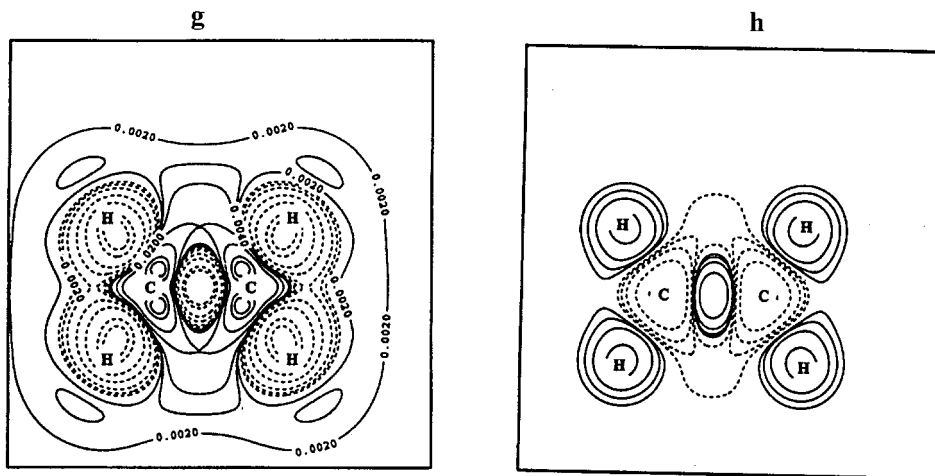
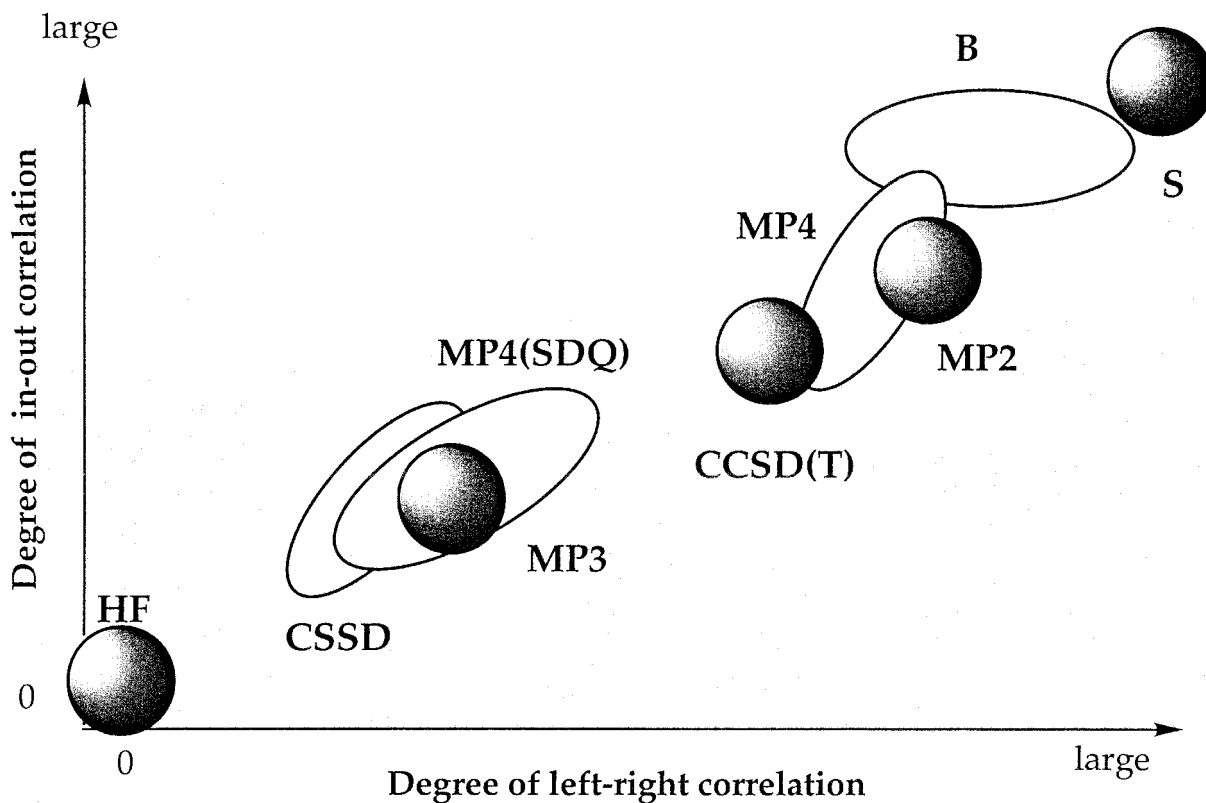
Figure 1. *Continued.*

Figure 2. Schematic representation of the degree of left-right and in-out pair correlation effects for different WFT and DFT methods [41]. For different molecules the sequence of methods is changed, which is indicated by overlapping areas.

in-out separation of negative charge for all molecules investigated in this work (figure 1(g)). However, the level of pair correlations is still lower than that calculated at the MP2 level of theory, as the difference density $\Delta\rho(\text{MP4} - \text{MP2}) = \rho(\text{MP4}) - \rho(\text{MP2})$ reveals (not shown, but see figure 2 for a qualitative assessment of pair correlation effects [44]). T effects are exaggerated at

the MP4 level of theory [6, 18, 19], which can be (partially) avoided by using CCSD(T). CCSD(T) includes DT, TT and other T coupling effects, which help to avoid an exaggeration of three-electron correlation as occurs at the MP4 level. Hence, the degree of left-right and in-out correlation covered at CCSD(T) is lower than that of both MP4 and MP2 (figures 1(h)

and 2); however, clearly it is larger than that at the MP3, MP4(SDQ) or CCSD levels.

We note in this connection that figure 2 gives only the degree of pair correlation. If the degree of three-electron correlation would be given on a third axis, MP2 would be at the zero point while CCSD(T) would be at a point along this axis representing about 77% of all three-electron correlation effects [18, 19]. Hence, it is not a contradiction that MP2 covers more pair correlation effects than does CCSD(T). (The mechanisms of two- and three-electron correlation are basically different, but both can lead to a left–right (angular, in–out) separation of negative charge. We simplify the description by considering these effects as a result of pair correlation.)

The stepwise addition of higher order correlation effects in MP or CC theory can lead to an oscillation of molecular properties and typical features of the electron density distribution, which has been observed also for many other molecules and molecular properties [6, 12, 13, 17]. Figures 1 and 2 provide a list of typical electron correlation effects that are used in the following to analyse electron correlation covered by DFT and SIC-DFT.

3.3. Correlation effects covered by DFT exchange functionals

It has been pointed out that exchange-only DFT methods already cover a larger amount of left–right electron correlation effects than WFT methods such as MP or CC [11]. In the case of the CO molecule, it was found that the B-only density distribution is close to that of the MP4 density distribution. This is confirmed by the results obtained in this work. For all molecules investigated, the B-only density is close to those of MP4, MP2, or CCSD(T) (see, e.g. figure 3(a)). The degree of left–right correlation suggested by the B-only density is in all cases considered larger than that covered by WFT methods (figure 2), raising the question whether a different type of pair correlation effect (non-dynamic rather than dynamic) is covered by exchange-only calculations. S exchange even increases the degree of pair correlation effects relative to that of B exchange (figures 3(b) and 2). The same is true for PW91-exchange (figure 3(c)), but differences between the two GGA functionals are of course much smaller than between the GGA functional B exchange and the LDA functional S exchange [11].

We need to determine why and in what way DFT exchange mimics left–right electron correlation effects, and for this purpose we consider first the influence of HF exchange on the electron density (figure 4(a) and table 1).

Exchange interactions between different electrons with aligned spins (interelectronic exchange) will be

small in those regions where (a) there is only little density (van der Waals regions), (b) only one electron can be expected (regions of the H atoms), and (c) electron pairing as in the CC bond region reduces the chance of finding a second electron of the same spin. (To assess the exchange interactions at the H atoms the CH bond polarity has to be considered: it is less likely to find a C electron at H than the H electron at C.) In those regions where exchange is small (large), Coulomb repulsion will be large (small), which leads to a decrease (increase) in the electron density. In agreement with these expectations, figure 4(a) (inter-electronic HF exchange in the molecular plane) reveals that density accumulates in the atomic regions and the non-bonded regions between the atoms. It is reduced in the bond regions, at the H atoms, and in the van der Waals regions.

Exchange is large in the valence region of the C atoms and in the non-bonded regions between the bonds because at the C atom there can be up to four valence electrons of the same spin and in the non-bonded regions there is no energy principle that requires $\alpha\beta$ spin coupling. Relatively large exchange guarantees that Coulomb repulsion is low, and therefore the density increases in regions of large exchange. Since this is primarily in the valence regions of the heavy atoms (C in figure 4(a)), one is reminded of the intraatomic Hund's rule, which implies that in a molecule the electrons in the valence region of a given atom possess the same spin to keep Coulomb repulsion low. There is also a relatively large exchange density in those parts of the bond region where σ and π densities overlap (figure 4(b), interelectronic HF exchange in the π plane) so that σ and π electrons of the same spin can be found, thus increasing exchange interactions and lowering Coulomb repulsion.

We note that self-exchange is generally large where the density is large (e.g. in the bond regions). Accordingly, self-exchange contracts the electron density by transferring negative charge from the van der Waals and non-bonded regions to the bond regions. This can be made visible by plotting the density resulting from the Coulomb self-repulsion $\sum J_{ii}$, which is just the mirror image of the exchange density (multiplication of the density given in figure 4(c) by -1).

According to the difference density diagrams in figure 4(d–f), interelectronic SIC-DFT exchange (also termed *correct DFT exchange* in the following. HF exchange is frequently called exact exchange in DFT to distinguish it from the approximate exchange of standard exchange functionals. To avoid any confusion with the term exact exchange, we shall use the term correct exchange if we consider SIC-X energies) can differ from interelectronic HF exchange in various ways: SIC-S determines exchange locally according to the value of the density,

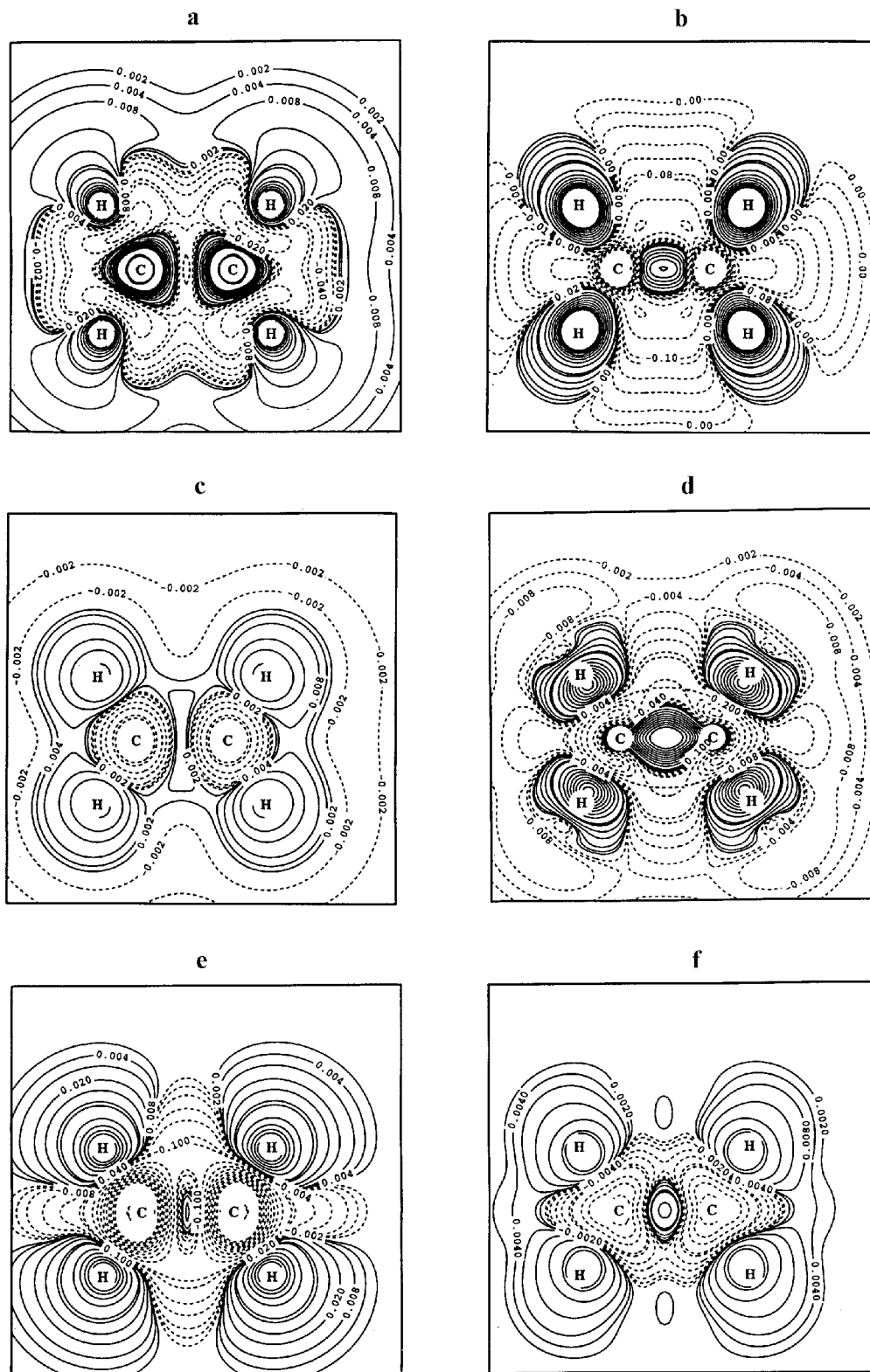


Figure 3. Contour line diagram of the difference electron density distribution $\Delta\rho(\mathbf{r}) = \rho(\text{method I}) - \rho(\text{method II})$ of ethene calculated with the cc-pVTZ basis in the experimental geometry. Solid (dashed) contour lines are in regions of positive (negative) difference densities. Reference plane is the plane containing the atoms. The positions of the atoms are indicated. The contour line levels have to be multiplied by the scaling factor 0.01 and are given in $e a_0^{-3}$. (a) B-only-MP4; (b) B-only-S-only; (c) B-only-PW91-only; (d) SIC-B-MP4; (e) SIC-B-SIC-S; and (f) SIC-B-SIC-PW91.

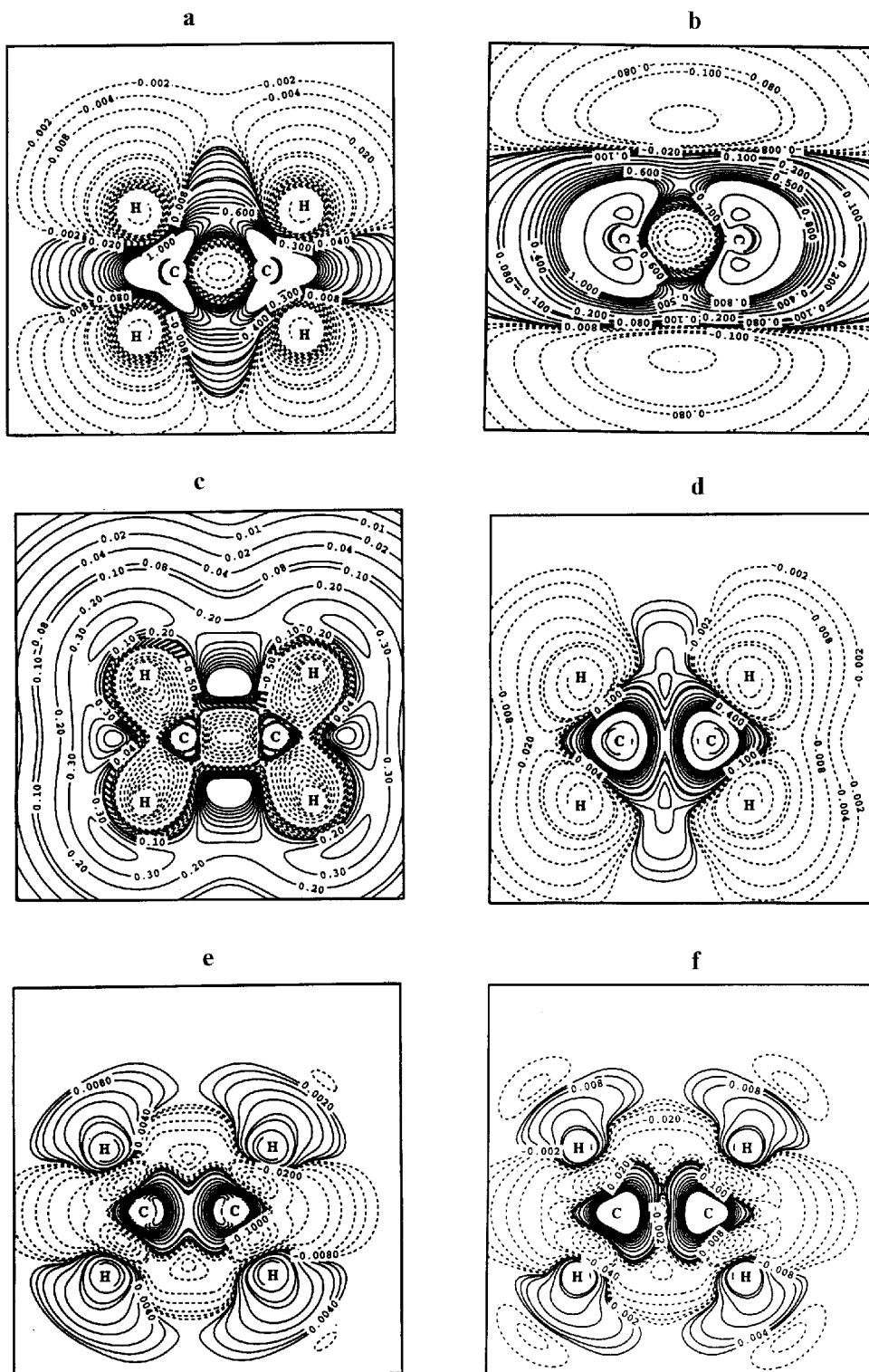


Figure 4. Contour line diagram of the difference electron density distribution $\Delta\rho(\mathbf{r}) = \rho(\text{method I}) - \rho(\text{method II})$ of ethene calculated with the cc-pVTZ basis in the experimental geometry. Solid (dashed) contour lines are in regions of positive (negative) difference densities. Reference plane, if not otherwise indicated, is the plane containing the atoms. The positions of the atoms are indicated. The contour line levels have to be multiplied by the scaling factor 0.01 and are given in $e a_0^{-3}$. (a) HF exchange; (b) HF exchange (plane perpendicular to the molecular plane and containing the C atoms); (c) HF, Coulomb self-repulsion; (d) SIC-S-HF exchange; (e) SIC-B-HF exchange; and (f) SIC-PW91-HF exchange. For definition of the difference densities, see table 1 and text.

i.e. high densities in the atomic and bonding regions automatically lead to relatively high exchange, which in turn causes an increase in the exchange densities to values larger than those found at the HF level of theory (figure 4(d), SIC-S–HF exchange). This is also true in the non-bonding regions where, because of a superposition of atomic density tails, the local approach automatically implies a higher exchange than HF exchange. We note in this connection that the magnitude of correct S exchange is larger than HF exchange (table 2), and that the common finding that S exchange underestimates the magnitude of exact exchange is just a consequence of the relatively large S-SIE.

The GGA functional B exchange also depends on the reduced density gradient [35], which is relatively large in the regions of the H atoms (relatively large gradient of the density for relatively small $\rho(\mathbf{r})$ values) and the C atoms (larger gradient, but also larger density) while it is smaller in the bond regions (small gradient), the outer non-bonded, and the van der Waals regions (figure 4(e), SIC-B–HF exchange). A direct comparison of the correct B and the correct S exchange densities (figure 3(e), SIC-B–SIC-S exchange) reveals that the former functional accumulates less density in the CC unit (valence region + bond region) than the SIC-S functional, which again reflects the influence of the reduced gradient of the density.

The SIC-PW91 exchange functional leads to small but significant changes relative to the SIC-B functional (figure 3(f), SIC-B–SIC-PW91 exchange). There is more density in the valence regions of the C atoms, but less in the CC bonding region and at the H atoms than calculated with SIC-B. We note that SIC-PW91 leads to a significantly larger absolute value of correct exchange than SIC-B, the two energies bracketing the HF exchange energies (exception H_2 , table 2).

In conclusion, the electron density distributions resulting from correct S, correct B, or correct PW91 exchange do not indicate any particular dynamic or non-dynamic electron correlation effects. All exchange densities overestimate the density in the CC unit (valence regions and bonding region), but provide different descriptions in other parts of the ethene molecule. If the SIC-B density is compared with WFT densities (see, e.g. figure 3(d), SIC-B–MP4), the same pattern of regions with density increase (CC unit and H atoms) and density decrease (CH bond regions, nonbonded regions, van der Waals region) will always be observed, even if the HF method is used for comparison. Since none of the correct DFT exchange functionals seems to cover any dynamic or non-dynamic electron correlation effects, we come to the surprising conclusion that the left–right correlation effects mimicked by standard

DFT exchange functionals are due to the SIE of these functionals.

3.4. Correlation effects covered by the DFT C functional

Dynamic electron correlation is described at the LDA level (e.g. by VWN, VWN5, etc.) by an attractive local potential that depends on the magnitude of the electron density. Hence, it is rather strong in the atomic, bond and (inner) non-bonded regions (superposition of atomic densities), but relatively weak in the van der Waals regions. LDA correlation functionals all lead to a transfer of electron density from regions with low electron density into regions with high electron density, as shown in figure 5(a) for the VWN5 correlation functional in the case of ethene. As the correlation potential depends on the local density only, this charge transfer will be less specific than the charge transfer due to the explicit inclusion of electron correlation effects by a WFT method.

The absolute magnitude of the LDA correlation energy is strongly exaggerated in this way: it is almost twice as large as the correct correlation energy (table 2). The major reason for this exaggeration is the SIE as is documented by the magnitude of VWN5-SIE energy in table 2 and the electron density changes caused by the VWN5-SIE functional (figure 5(d)), which are positive in the CC and CH bond regions but negative in the non-bonded and van der Waals regions. Since the VWN5 functional with its SIE is adjusted to the (SIE-free) quantum Monte Carlo description of the homogeneous electron gas, the relatively large VWN5-SIE leads to strong changes in the regions of relatively high density, as for example in the CC bonding region. SIC-VWN5 (figure 5(f)) similar to VWN5 (figure 5(a)) increases the density in all those regions where the value of the density is already significant, but decreases it in the CC bonding region due to the large SIC in this region (figure 5(f)).

In its construction the LYP correlation functional [36] does not suffer from an SIE. It predicts an increase in the electron density in the region of the CC unit and in the non-bonded regions between the H atoms (figure 5(b)). There is some similarity to the VWN5-SIC correlation density in so far as the increase in density covers the major part of the CC unit, but even for the SIC-VWN5 the increase in correlation density is still exaggerated, as is confirmed by the correct VWN5 correlation energy compared with the LYP correlation energy (table 2) and the larger region of positive correlation density. (The term correlation density is used in the same way as the term exchange density, i.e. the difference density of entry 13 in table 1 reflects the impact of the correlation functional on the density distribution, but does not

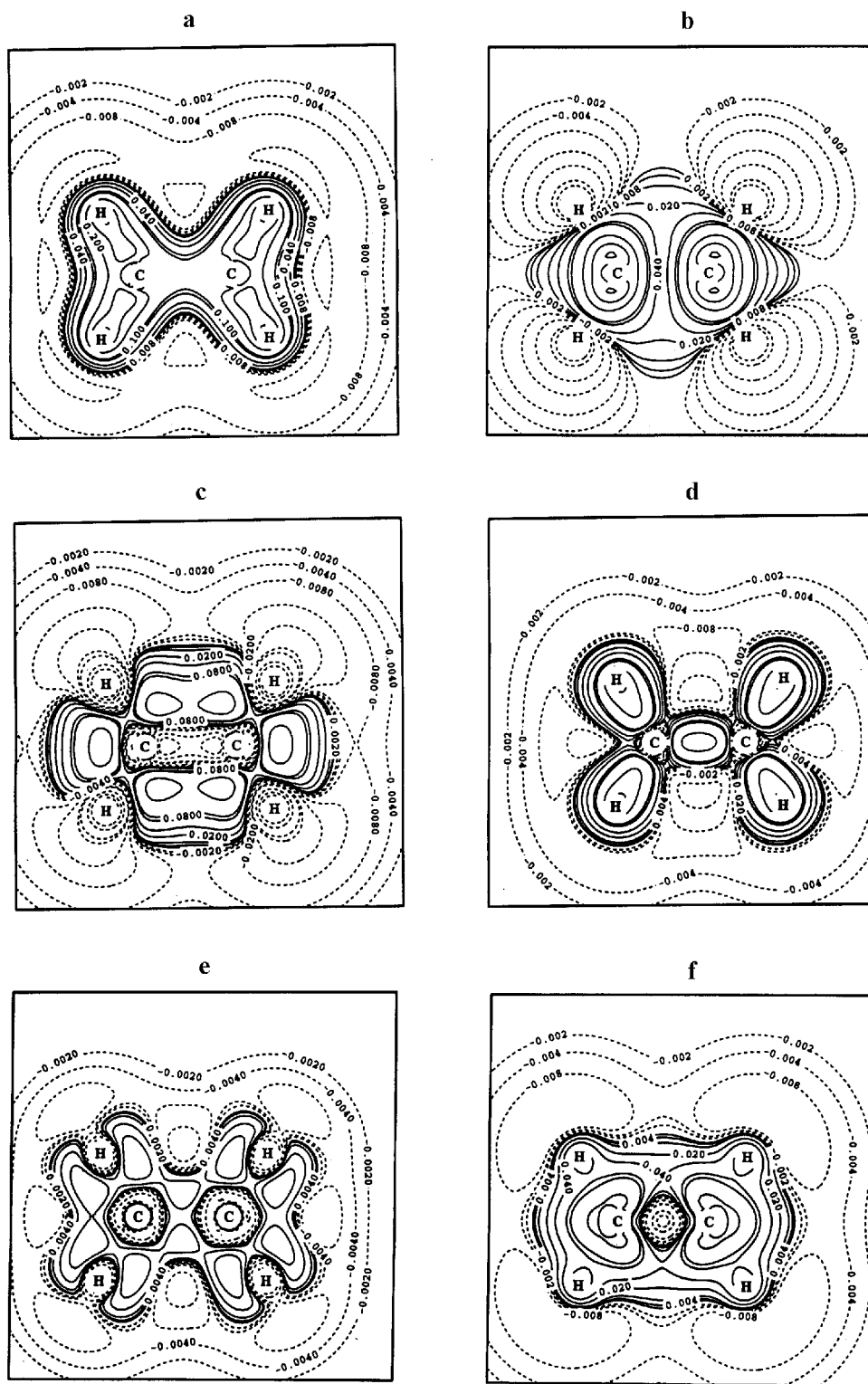


Figure 5. Contour line diagram of the electron density distribution of ethene calculated with the cc-pVTZ basis in the experimental geometry for various correlation functionals. Solid (dashed) contour lines are in regions of positive (negative) difference densities. Reference plane is the plane containing the atoms. The positions of the atoms are indicated. The contour line levels have to be multiplied by the scaling factor 0.01 and are given in $e a_0^{-3}$. (a) VWN5 functional; (b) LYP functional; (c) PW91 functional; (d) VWN5-SIE functional; (e) PW91-SIE functional; and (f) SIC-VWN5 functional. For definition of the difference densities, see table 1 and text.

represent the correct correlation energy density as defined in [32].)

The density of the PW91 correlation functional depends on the magnitude of both the density and its gradient. Since the gradient is smaller in the CC bonding region than in the non-bonded regions between the H atoms (exponential decay of $\rho(\mathbf{r})$) the PW91 correlation density is accumulated in the non-bonded regions but depleted in the CC bond region, at the H atoms, and in the van der Waals region (figure 5(c)). The density changes caused by the PW91-SIE partially enhance, partially oppose these effects (figure 5(e)), but changes are rather small (one third of the changes caused by VWN5-SIE, table 2) so that the overall pattern of the correlation density caused by PW91-SIC (not shown) is similar to that caused by PW91. Hence, VWN5 and LYP increase, PW91 decreases the CC bond density. In all cases, non-bonded interactions become stronger due to an increase in the correlation density, while the density in the van der Waals region is always reduced.

4. The role of the self-interaction error

The Coulomb self-repulsion of the electrons (reflected by the difference density described under entry 1 of table 1) removes density out of the space with large amplitudes of the orbitals φ_i into the regions with small amplitudes of orbitals φ_i , i.e. for molecules from the bond regions into the non-bonded and van der Waals regions (figure 4(c)). HF self-exchange has just the opposite effect, i.e. it transfers density from non-bonded and van der Waals regions into the bond regions. If at the DFT level Coulomb self-interaction is larger than exchange self-interaction in the bond region, which is always true because the magnitude of total exchange is relatively small there (see figure 4(a) and discussion in §3), density is removed artificially out of the bond regions by the resulting X-SIE, thus simulating left-right correlation and other pair correlation effects. These effects are even larger than the exaggerated description of pair correlation effects obtained at the MP2 level (figure 2; figure 1(a), MP2-HF) because the former are related to long range rather than just short range pair correlation.

In passing we note that various authors have pointed out in the past that DFT exchange covers also non-dynamic electron correlation effects. For example, Becke [44, 45] emphasized this point when comparing the delocalized character of the HF exchange hole with the localized DFT exchange hole attached to the reference electron. Also, Baerends and coworkers [46–48], studying exchange potentials and exchange energy densities derived from high level WFT methods, came to the conclusion that GGA exchange must contain non-dynamic electron correlation effects. Gräfenstein *et al.*

[49] pointed out that for both WFT and DFT methods exchange can cover non-dynamic electron correlation. In SIC-DFT investigations of H_2 [50] and the $\text{H}_2 + \text{H}$ reaction system [51] observations have been made that seem to point in the same direction. In a recent paper by Handy and Cohen [42] the conclusion was drawn that exchange and left-right (long range) electron correlation are entangled and cannot be separated.

Exchange holes tend to be delocalized in molecules, as was first pointed out by Slater [33, 52] and later emphasized by various authors [44–48]. This holds in particular for the self-exchange, as can be demonstrated in the case of the H_2 molecule, for which exchange is just the one-electron cancellation term for Coulomb self-interaction and the exchange hole just the negative of the σ_g orbital density [53]. Hence, the exchange hole is delocalized over the whole bond region, independent of the position of the reference electron, and does not reflect any short range or long range electron correlation effects. The electron density related to the H_2 self-exchange hole is large close to the nuclei (deep exchange hole) and smaller in the bond region (flat exchange hole). If the reference electron moves out into the van der Waals region, the exchange hole will not follow, but will stay behind in regions of higher densities.

The DFT exchange hole is by construction localized, spherically symmetric, depends on the position of the reference electron, and seems to cover long range (i.e. non-dynamic) pair correlation effects. If the reference electron with spin σ is close to the left nucleus, causing a concentric DFT hole located at this position, then there is a relatively large probability of finding the second electron close to the right nucleus, although the HF and SIC-DFT exchange holes give a low probability of finding the second electron close to the right nucleus. Hence, the difference between the DFT and the SIC-DFT (HF) exchange holes, namely the SIE part of the DFT exchange hole, leads to a strongly increased probability of long range left-right correlation: reference electron close to the left nucleus, second electron close to the right nucleus. Another way to describe the role of the SIE is to consider the fact that DFT imposes a localized exchange hole whereas the exact exchange hole is delocalized, reflecting details of the electronic structure. The SIE part annihilates the delocalized structure of the correct exchange hole to obtain a localized one, thus introducing long range correlation effects. Since normal long range left-right correlation is a result of Coulomb interactions for two particles with equal or opposite spin, and since exchange interactions and exchange holes have different physical origins, it is appropriate to say that the SIE part of the DFT exchange hole mimics (rather than causes) long range correlation effects. The latter are responsible for the

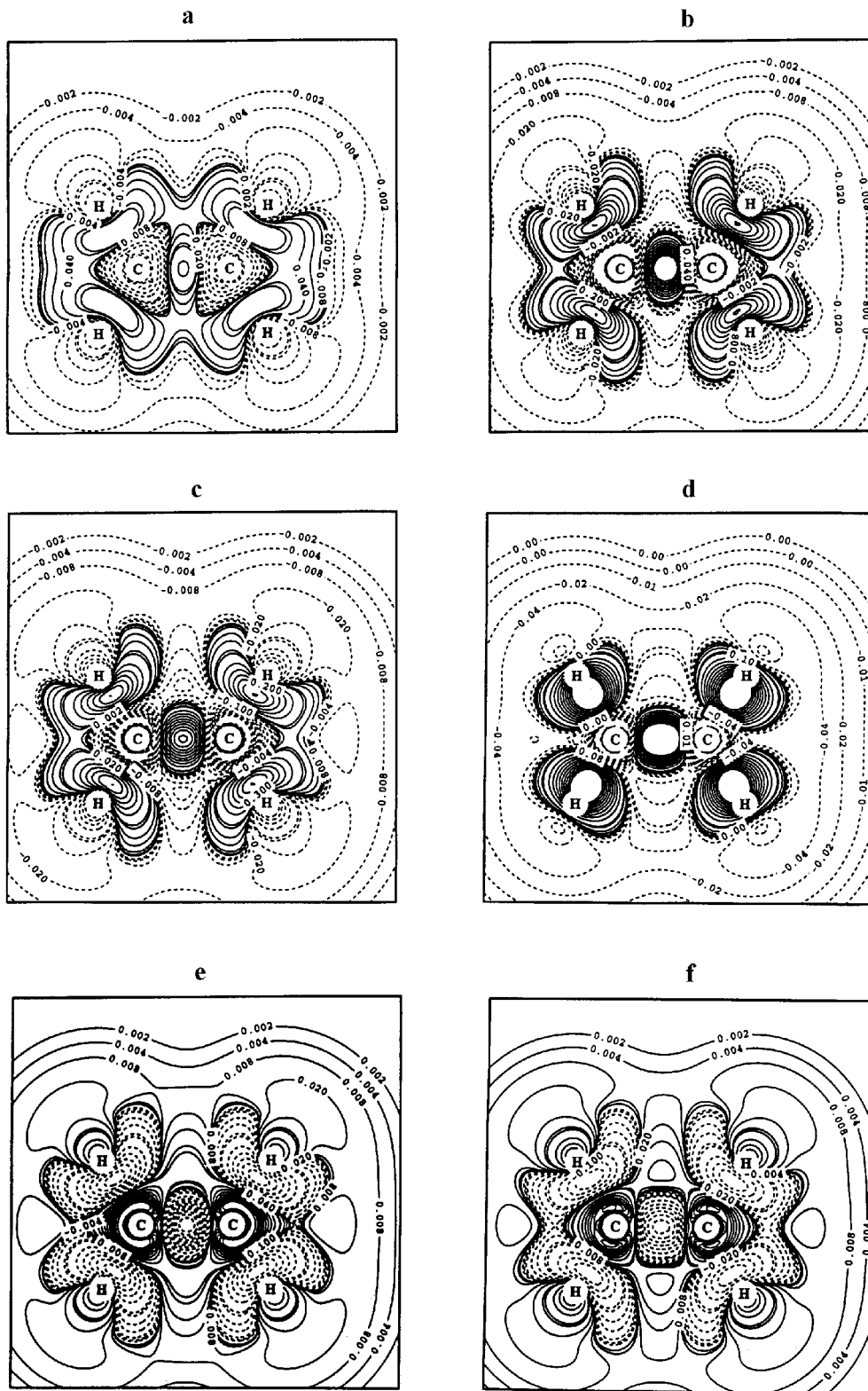


Figure 6. Contour line diagram of the difference electron density distribution $\Delta\rho(\mathbf{r}) = \rho(\text{method I}) - \rho(\text{method II})$ of ethene calculated with the cc-pVTZ basis in the experimental geometry. Solid (dashed) contour lines are in regions of positive (negative) difference densities. Reference plane is the plane containing the atoms. The positions of the atoms are indicated. The contour line levels have to be multiplied by the scaling factor 0.01 and are given in $e a_0^{-3}$. (a) B3LYP-BLYP; (b) SIC-BLYP-BLYP; (c) SIC-PW91PW91-PW91PW91; (d) SIC-SVWN5-SVWN5; (e) B3LYP-SIC-BLYP; and (f) B3PW91-SIC-PW91PW91.

changes in the electron density distribution caused by the SIE. For example, density is removed from the bond region and accumulated in the valence regions of the atoms (see figure 6(b)), SIC-BLYP–BLYP, this gives the SIC of B exchange; the corresponding SIE = –SIC is obtained by multiplying the difference density of figure 6(b) by –1).

Clearly, little long range correlation is needed to describe a closed shell molecule such as ethene, and therefore the SIE may exaggerate non-dynamic electron correlation. The SIE of the correlation functionals, VWN5-SIE and PW91-SIE, partially corrects the artificial exaggeration of long range pair correlation. The DFT correlation hole, which is also localized and connected to the reference electron, introduces short range correlation effects that make it possible for the density to be contracted to regions out of which density is removed by long range electron correlation simulated by the X-SIE. For example, density moves from the non-bonded and van der Waals regions to the bond regions. However, DFT correlation effects are less than 10% of the exchange effects, so that long range pair correlation effects are still exaggerated by the exchange–correlation functional. The C-SIE enhances these effects, which could be viewed as if the C-SIE narrows the radius of the correlation hole, thus localizing it further and compensating for a smaller part of the long range effects of X-SIE. SIC-C functionals concentrate density to a lesser extent in the bond region, as is shown, e.g. in figure 5(f) (SIC-VWN5). Clearly the total effect of SIC is dominated by SIC-X: for SIC-BLYP, SIC-SVWN5 or SIC-PW91PW91 (figure 6(b–d)), the density is moved back from the non-bonded and van der Waals regions to the bond region, thus cancelling somewhat the long range pair correlation effects.

We have observed such effects also for the hybrid functionals (figure 6(a), B3LYP–BLYP) [11]. For all molecules investigated the general pattern of the difference density $\Delta\rho(\text{B3LYP}/\text{BLYP}) = \rho(\text{B3LYP}) - \rho(\text{BLYP})$ is similar to that of the difference density $\Delta\rho(\text{SIC-XC}/\text{XC}) = \rho(\text{SIC-XC}) - \rho(\text{XC})$ (XC is BLYP, PW91PW91, SVWN5, figure 6(b–d)) where in general changes caused by the hybrid functional are smaller than those caused by the corresponding SIC-XC functional (figures 6(e), B3LYP–SIC-BLYP; figure 6(f), B3PW91–SIC-PW91PW91).

By their construction, hybrid functionals incorporate some exact exchange and, by this, a more delocalized exchange hole that compensates for some of the long range pair correlation effects of the SIE part of the local exchange hole [38]. Hence, the use of hybrid functionals can be viewed as partially correcting for the SIE and the associated long range correlation effects of stan-

dard exchange functionals in an empirical way. As noted previously, these corrections remind one of the inclusion of coupling between n -electron (diagonal) correlation effects at the WFT level of theory [11]. Diagonal correlation effects such as 2, 3, 4, ..., n -electron correlation effects expand the density (transfer of negative charge from bonding to non-bonding regions) while the coupling between the diagonal correlation terms reduces the expansion of the electron density and increases the density in the bond regions [16–19]. In general, one can say that the inclusion of higher order electron correlation (where higher order implies both increase in the number of correlating electrons and increase in the number of coupling effects) often reduce those effects resulting from low order electron correlation. Both the hybrid and the SIC-XC functionals mimic these higher order correlation effects. In view of the insight gained in this work, we can refine this picture by saying that changes at the DFT level of theory are much stronger because (partial or full) cancellation of long range (non-dynamic) correlation effects implies larger changes in the density than observed for WFT methods.

There is a substantial difference between hybrid and SIC-XC functionals. The former are calibrated to reproduce experimental heats of formation [38]; despite the admixture of HF exchange, they cover a residual SIE, which is reflected in the difference density plots of figure 6(e) and (f). Correcting for this residual SIE does not necessarily imply an improvement of molecular properties calculated with the SIE-free hybrid functional. We may conclude that the SIC-XC functionals themselves will not lead to a substantial improvement in calculated molecular properties, because the exchange–correlation functionals were optimized in the presence rather than the absence of the corresponding SIE. Exceptions will be found in those cases where, as a consequence of the electronic structure, strongly delocalized exchange holes are absolutely important. It has been found that for the case of 1- or 3-electron bonds (radical cations, etc.), SIC-DFT methods perform considerably better than standard DFT methods using either GGA or hybrid functionals [54]. Baerends and coworkers [47] have given a generalization of these cases and new exchange functionals based on delocalization indicators have been developed to account for these situations without requiring the costly inclusion of an SIE correction [55].

5. Conclusion

The magnitude of the SIE is different for different functionals. It is positive and about 13–15% of correct exchange in the case of the S functional, negative and 1–2% of correct exchange for the B functional, and positive and less than 1% for the PW91 functional. The

impact of the SIE is even larger for the correlations functionals VWN5 (about 45% of correct correlation) and PW91 (about 24%), where its value is always negative, i.e. correlation is exaggerated. This leads in the case of the SVWN5 functional to some cancellation of the X-SIE; however, since the latter dominates (electron interactions due to exchange are more than 95% of the total exchange–correlation interaction energy) the total SIE is still large. For the GGA functionals the SIE is relatively small but still significant. The best agreement between HF exchange and GGA exchange is found for PW91. The PW91PW91 functional leads to the smallest SIE.

For all the molecules investigated in this work the exchange functionals mimic effects that are actually reminiscent of pair- and three-electron correlation effects introduced by MP2 and MP4 in WFT. Indeed, the best agreement between B only and WFT calculations is found with MP4, and somewhat less with MP2 and CCSD(T). However, clearly left–right correlation and in–out correlation are exaggerated by B exchange and even more by S exchange (figure 2).

The correlation effects simulated by the exchange functionals are a direct consequence of the X-SIE and they are of long range rather than short range nature as the comparison with the WFT might suggest. Analysis of the properties of the exchange hole for exact exchange (delocalized exchange hole) and for DFT exchange (localized hole) reveals that the X-SIE compensates for the delocalized structure of the self-interaction corrected exchange hole to yield the standard DFT exchange hole with localized character.

SIC-B densities do not reveal any correlation effects and therefore are closer to densities reflecting exact exchange. Compared with WFT densities they lead to a typical difference density pattern: accumulation in the bond regions, depletion in the non-bonded and van der Waals regions. SIC-PW91 and SIC-S lead to similar density changes.

Most correlation functionals contract the density towards the bond and valence region, thus taking negative charge out of the van der Waals region and improving the description of van der Waals interactions. The PW91 correlation functional follows largely these trends, but causes a reduction in density in heavy atom bonds, which is reminiscent of pair correlation effects.

SIC-C functionals such as SIC-VWN5 or SIC-PW91 possess less density in the bond regions and more in the non-bonded and van der Waals regions, because the C-SIE is responsible for a substantial part of the electron contraction observed for C functionals.

Hybrid functionals such as B3LYP increase the contraction of the electron density towards the bond regions. In this way higher order coupling between diagonal correlation effects is mimicked. The balanced

mixing (achieved by fitting DFT results to empirical data) of local and non-local exchange (besides 20–25% HF exchange) and correlation leads to a strengthening of heavy atom bonds so that B3LYP mostly gives the best account of all DFT methods. This is also reflected by the fact that often B3LYP densities are close to CCSD(T) densities [11].

SIC-XC functionals have a similar impact on the electron density distribution as hybrid functionals, which simply reflects the fact that the admixture of HF exchange and the calibration of the hybrid functionals with experimental data compensates for a large part of the SIE of standard exchange–correlation functionals.

In view of the results obtained in this work one can consider hybrid functionals as the poor man's approach to SIC-DFT. Routine application of SIC-DFT is far too costly, because its cost increases with the number of electrons in a molecule. Also, there is little sense in carrying out SIC-DFT calculations with standard exchange–correlation functionals because the latter were calibrated for DFT methods that included SIEs. Hence, one has to readjust standard functionals to SIC-DFT to develop more accurate DFT methods.

Several authors have discussed the related nature of exchange and long range correlation from different points of view [42, 44–49]. Handy and Cohen [42] summarized these discussions in the sentence 'exchange and left–right correlation cannot be separated', although they have different physical origin. All authors agree that long range correlation effects are mimicked in the case of DFT by the localized character of the DFT exchange hole. In the present work, we make one additional step in the discussion by focusing on the SIE of DFT exchange and clarifying that this is actually responsible for the inclusion of non-dynamic electron correlation into DFT exchange. Work is in progress to clarify consequences of these findings when investigating electronic systems with distinct multireference character.

This work was supported at Göteborg by the Swedish Natural Science Research Council (NFR) with financial support. Calculations were done on the supercomputers of the Nationellt Superdatorcentrum (NSC), Linköping, Sweden. D.C. and E.K. thank the NSC for a generous allotment of computer time.

References

- [1] HOHENBERG, P., and KOHN, W., 1994, *Phys. Rev. B*, **136**, 864.
- [2] KOHN, W., and SHAM, L., 1965, *Phys. Rev. A*, **140**, 1133.
- [3] For reviews on DFT methods, see, e.g., PARR, R. G., and YANG, W., 1989, *Density-Functional Theory of Atoms and Molecules* (Oxford University Press), 1990, edited by Labanowski, J. K., and ANDZELM, J. W., 1990, *Density Functional Methods in Chemistry* (Heidelberg: Springer-

- Verlag); Seminario, J. M. Politzer, P., 1996, *Modern Density Functional Theory—A Tool For Chemistry* (Amsterdam: Elsevier); CHONG, D. P., 1995, *Recent Advances in Density Functional Methods*, Part II (Singapore: World Scientific); Dobson, J. F., Vignale, G. and Das, M. P., 1997, *Electronic Density Functional Theory, Recent Progress and New Directions* (New York: Plenum Press); LÖWDIN, P.-O., 1999, *Advances in Quantum Chemistry, Density Functional Theory* (New York: Academic Press).
- [4] See, e.g., LAIRD, B. B., ROSS, R. B., and ZIEGLER, T., 1996, *Chemical Applications of Density Functional Theory* (Washington, DC: American Chemical Society); JOUBERT, D., 1997, *Density Functionals: Theory and Applications* (Heidelberg: Springer-Verlag); GILL, P., 1998, *Encyclopedia of Computational Chemistry*, Vol. 1, edited by P.v.R. Schleyer, N. L. Allinger, T. Clark, J. Gasteiger, P. A. Kollman, H. F. Schaefer III, and R. Schreiner (Chichester: Wiley) p. 678 and references therein; see also Kraka, E., Sosa, C. P. and Cremer, D., 1996, *Chem. Phys. Lett.*, **260**, 43; Gutbrod, R., Kraka, E., Schindler, R. N. and Cremer, D., 1997, *J. Amer. chem. Soc.*, **119**, 7330; Gräfenstein, J., Cremer, D., and Kraka, E., 1998, *Chem. Phys. Lett.*, **288**, 593; Cremer, D., Kraka, E., and Szalay, P. G., 1998, *Chem. Phys. Lett.*, **292**, 97; Kraka, E., and Cremer, D., 2000, *J. Amer. chem. Soc.*, **122**, 8245.
- [5] MÖLLER, C., and PLESSET, M. S., 1934, *Phys. Rev.*, **46**, 618.
- [6] For a recent review see, CREMER, D., 1998, *Encyclopedia of Computational Chemistry*, Vol. 3, edited by P.v.R. Schleyer, N. L. Allinger, T. Clark, J. Gasteiger, P. A. Kollman, H. F. Schaefer III, and P. R. Schreiner (Chichester: Wiley) p. 1706.
- [7] For recent reviews see CRAWFORD, T. D., and SCHAEFER, III, H. F., 2000, *Reviews in Computational Chemistry*, Vol. 14, edited by K. B. Lipkowitz, and D. B. Boyd (Weinheim: Verlag Chemie) p. 33; Gauss, J., 1998, *Encyclopedia of Computational Chemistry*, Vol. 1, edited by P.v.R. Schleyer, N. L. Allinger, T. Clark, J. Gasteiger, P. A. Kollman, H. F. Schaefer III, and P. R. Schreiner, (Chichester: Wiley) p. 615.
- [8] BARTLETT, R. J., and STANTON, J. F., 1994, *Reviews in Computational Chemistry*, Vol. 5, edited by K. B. Lipkowitz, and D. B. Boyd, (Weinheim: Verlag Chemie) p. 65; Cremer, D., and He, Z., 1997, *Conceptual Perspectives in Quantum Chemistry*, Vol. III, edited by J.-L. Calais, and E. Kryachko, (Dordrecht: Kluwer) p. 239.
- [9] PURVIS III, G. D., and BARTLETT, R. J., 1982, *J. chem. Phys.*, **76**, 1910.
- [10] RAGHAVACHARI, K., TRUCKS, G. W., POPLE, J. A., and HEAD-GORDON, M., 1989, *Chem. Phys. Lett.*, **157**, 479.
- [11] HE, Y., GRÄFENSTEIN, J., KRAKA, E., and CREMER, D., 2000, *Molec. Phys.*, **98**, 1639.
- [12] KRAKA, E., GAUSS, J., and CREMER, D., 1991, *J. molec. Struct. Theochem*, **234**, 95.
- [13] GAUSS, J., and CREMER, D., 1992, *Adv. Quantum Chem.*, **23**, 205.
- [14] HE, Z., and CREMER, D., 1996, *Intl. J. Quantum Chem.*, **59**, 15, 31, 57, 71.
- [15] CREMER, D., and HE, Z., 1996, *J. phys. Chem.*, **100**, 6173; 1997, *J. molec. Struct. Theochem*, **398–399**, 7.
- [16] HE, Y., and CREMER, D., 2000, *Molec. Phys.*, **98**, 1415.
- [17] FORSBERG, B., HE, Z., HE, Y., and CREMER, D., 2000, *Intl. J. Quantum Chem.*, **76**, 306.
- [18] HE, Z., and CREMER, D., 1991, *Intl. J. Quantum Chem. Symp.*, **25**, 43.
- [19] HE, Z., and CREMER, D., 1993, *Theoret. Chim. Acta*, **85**, 305.
- [20] LINDGREN, I., 1971, *Intl. J. Quantum Chem. Symp.*, **5**, 411; PERDEW, J. P., 1979, *Chem. Phys. Lett.*, **64**, 127.
- [21] PERDEW, J. P., and ZUNGER, A., 1981, *Phys. Rev. B*, **23**, 5048.
- [22] PERDEW, J. P., 1984, *Local Density Approximations in Quantum Chemistry, and Solid State Physics*, edited by J. Avery, and J. P. Dahl (New York: Plenum Press); Perdew, J. P., and Ernzerhof, M., 1998, *Electronic Density Functional Theory: Recent Progress, and New Directions*, edited by J. F. Dobson, G. Vignale, and M. P. Das (New York: Plenum Press) p. 31.
- [23] LUNDIN, U., and ERIKSSON, O., 2001, *Intl. J. Quantum Chem.*, **81**, 247; BIAGINI, M., 1994, *Phys. Rev. B*, **49**, 2156; SVANE, A., 1995, *Phys. Rev. B*, **51**, 7924. BIAGINI, M., 1995, *Phys. Rev. B*, **51**, 7927.
- [24] HARRISON, J. G., HEATON, R. A., and LIN, C. C., 1983, *J. Phys. B*, **16**, 2079; Pederson, M. R., Heaton, R. A., and Lin, C. C., 1984, *J. chem. Phys.*, **80**, 1972; Svane, A., Temmerman, W. M., Szotek, Z., Laegsgaard, J., and Winter, H., 1999, *Intl. J. Quantum Chem.*, **77**, 799; Goedecker, S., and Umrigter, C. J., 1977, *Phys. Rev. A*, **55**, 1765.
- [25] GUO, Y., and WHITEHEAD, M. A., 1991, *J. comput. Chem.*, **12**, 803. CHERMETTE, H., CIOFINI, I., MARIOTTI, F., and DAUL, C., 2001, *J. chem. Phys.*, **114**, 1447.
- [26] LI, Y., and KRIEGER, J. B., 1990, *Phys. Rev. A*, **41**, 1701. GILL, P. M. W., JOHNSON, B. G., GONZALES, C. A., and POPLE, J. A., 1994, *Chem. Phys. Lett.*, **221**, 100; WHITEHEAD, M. A., and SUBA, S., 1995, *Recent Advances in Density Functional Methods*, Part I, edited by D. P. Chong, (Singapore: World Scientific) p.53; Chen, J., Krieger, J. B., and Li, Y., 1996, *Phys. Rev. A*, **54**, 3939; Garza, J., Nichols, J. A., and Dixon, D. A., 2000, *J. chem. Phys.*, **112**, 7880; **113**, 6029; Garza, J., Vargas, R., Nichols, J. A., and Dixon, D. A., 2001, *J. chem. Phys.*, **114**, 639.
- [27] FERMI, E., and AMALDI, E., 1934, *Accad. Ital. Rome*, **6**, 117.
- [28] POLO, V., KRAKA, E., and CREMER, D., unpublished.
- [29] PEDERSON, M. R., and LIN, C. C., 1988, *J. chem. Phys.*, **88**, 1807.
- [30] See compilation of experimental geometries in HEHRE, W. J., RADOM, L., SCHLEYER, P.v.R., and POPLE, J., 1985, *Ab Initio Molecular Orbital Theory* (New York: Wiley); specific geometries: H₂, O₂ in Huber, K. P., and Herzberg, G. H., 1979, *Molecular Spectra and Molecular Constants of Diatomic Molecules* (New York: Van Nostrand-Reinhold); C₂H₆ in Hirota, E., Endo, Y., Saito, S., and Duncan, J. L., 1981, *J. molec. Spectrosc.*, **89**, 285; C₂H₄ in Hirota, E., Endo, Y., Saito, S., Yoshida, K., Yamaguchi, I., and Machida, K., 1983, *J. molec. Spectrosc.*, **89**, 223; C₂H₂ in Kostyk, E., and Welsh, H. L., 1980, *Can. J. Phys.*, **58**, 912; N₂H₂ in Demaison, J., Hegelung, F., and Buerger, H., 1997, *J. molec. Struct.*, **413**, 447; N₂ in Orlov, M. L., Ogilvie, J. F., and Nibler, J. W., 1997, *J. molec. Spectrosc.*, **185**, 128; H₂O₂ in Pelz, G., Yamada, K. M. T., and Winnewisser, G., 1993, *J. molec. Spectrosc.*, **159**, 507; F₂ in Edwards, A., Goods, B., and Long, C.,

- 1976, *J. chem. Soc. Faraday Trans ii*, **72**, 984; CO in Authier, N., Bagland, N., and Le Floch, A., 1993, *J. molec. Spectrosc.*, **160**, 590.
- [31] DUNNING JR., T. H., 1989, *J. chem. Phys.*, **99**, 1007.
- [32] BURKE, K., CRUZ, F. G., and LAM, K., 1998, *J. chem. Phys.*, **109**, 8161.
- [33] SLATER, J., 1951, *Phys. Rev.*, **81**, 385.
- [34] VOSKO, S. H., WILK, L., and NUSAIR, M., 1980, *Can. J. Phys.*, **58**, 1200.
- [35] BECKE, A. D., 1988, *Phys. Rev. A*, **38**, 3098.
- [36] LEE, C., YANG, W., and PARR, R. G., 1988, *Phys. Rev. B*, **37**, 785.
- [37] PERDEW, J. P., 1991, *Electronic Structure of Solids '91*, edited by P. Ziesche, and H. Eschrig, (Berlin: Akademie-Verlag) p. 11; PERDEW, J. P., and WANG, Y., 1992, *Phys. Rev. B*, **45**, 13244.
- [38] BECKE, A. D., 1993, *J. chem. Phys.*, **98**, 5648.
- [39] KRAKA, E., GRÄFENSTEIN, J., GAUSS, J., REICHEL, F., OLSSON, L., KONKOLI, Z., HE, Z., and CREMER, D., 2000, Cologne 2000, Göteborg University, Göteborg.
- [40] FRISCH, M. J., TRUCKS, G. W., SCHLEGEL, H. B., SCUSERIA, G. E., ROBB, M. A., CHEESEMAN, J. R., ZAKRZEWSKI, V. G., MONTGOMERY JR., J. A., STRATMANN, R. E., BURANT, J. C., DAPPRICH, S., MILLAM, J. M., DANIELS, A. D., KUDIN, K. N., STRAIN, M. C., FARKAS, O., TOMASI, J., BARONE, V., COSSI, M., CAMMI, R., MENNUCCI, B., POMELLI, C., ADAMO, C., CLIFFORD, S., OCHTERSKI, J., PETERSSON, G. A., AYALA, P. Y., CUI, Q., MOROKUMA, K., MALICK, D. K., RABUCK, A. D., RAGHAVACHARI, K., FORESMAN, J. B., CIOSLOWSKI, J., ORTIZ, J. V., STEFANOV, B. B., LIU, G., LIASHENKO, A., PISKORZ, P., KOMAROMI, I., GOMPERS, R., MARTIN, R. L., FOX, D. J., KEITH, T., AL-LAHAM, M. A., PENG, C. Y., NANAYAKKARA, A., GONZALEZ, C., CHALLACOMBE, M., GILL, P. M. W., JOHNSON, B., CHEN, W., WONG, M. W., ANDRES, J. L., GONZALEZ, C., HEAD-GORDON, M., REPLOGLE, E. S., and POPLE, J. A., 1998, Gaussian98, Revision A3 (Pittsburgh, PA: Gaussian, Inc.).
- [41] STANTON, J. F., GAUSS, J., WATTS, J. D., LAUDERDALE, W. J., and BARTLETT, R. J., 1992, Aces II, Quantum Theory Project (University of Florida); see also STANTON, J. F., GAUSS, J., WATTS, J. D., LAUDERDALE, W. J., and BARTLETT, R. J., 1992, *Intl. J. Quantum Chem. Symp.*, **26**, 879.
- [42] HANDY, N. C., and COHEN, A. J., 2001, *Molec. Phys.*, **99**, 403.
- [43] CREMER, D., 2001, *Molec. Phys.*, **99**, 1899.
- [44] BECKE, A. D., 1995, *Modern Electronic Structure Theory*, Part II, edited by D. R. Yarkony, (Singapore: World Scientific) p. 1022.
- [45] BECKE, A. D., 1996, *J. chem. Phys.*, **104**, 1040.
- [46] GRITSENKO, O. V., SCHIPPER, P. R. T., and BAERENDS, E. J., 1997, *J. chem. Phys.*, **107**, 5007.
- [47] GRITSENKO, O. V., ENSING, B., SCHIPPER, P. R. T., and BAERENDS, E. J., 2000, *J. phys. Chem. A*, **104**, 8558.
- [48] SCHIPPER, P. R. T., GRITSENKO, O. V., and BAERENDS, E. J., 1998, *Phys. Rev. A*, **57**, 1729.
- [49] GRÄFENSTEIN, J., HJERPE, A. M., KRAKA, E., and CREMER, D., 2000, *J. phys. Chem. A*, **104**, 1748;
- [50] CSOSKA, G. I., NGUYEN, N. A., and KOLOSSVARY, I., 1997, *J. comput. Chem.*, **12**, 1534.
- [51] CSOSKA, G. I., and JOHNSON, B. G., 1998, *Theoret. Chem. Accounts*, **99**, 158.
- [52] SLATER, J. C., 1974, *The Self-Consistent Field for Molecules, and SOLIDS* (New York: McGraw-Hill).
- [53] See, e.g., BAERENDS, E. J., and GRITSENKO, O. V., 1997, *J. phys. Chem. A*, **101**, 5390.
- [54] BALLY, T., and SASTRY, G. N., 1997, *J. phys. Chem. A*, **101**, 7923; SODUPE, M., BERTRAN, J., RODRIGUEZ-SANTIAGO, L., and BAERENDS, E. J., 1999, *J. phys. Chem. A*, **103**, 166; see also ZHANG, Y., and YANG, W., 1998, *J. chem. Phys.*, **109**, 2604, and [26].
- [55] See, e.g., BECKE, A., 2000, *J. chem. Phys.*, **112**, 4020 and references therein.